

Crack paths in a borosilicate glass under triaxial loading

V. Doquet, N. Ben Ali, A. Constantinescu

Laboratoire de mécanique des Solides, CNRS, Ecole Polytechnique, 91128 Palaiseau cedex,
France, doquet@lms.polytechnique.fr

ABSTRACT. *The growth of 3D star-like cracks in a porous borosilicate glass, with a “mirror- mist- hackle” aspect due to the dynamic character of their propagation was induced in cylindrical specimens by “cold-to-hot” thermal shocks inducing triaxial tension. Pores were identified as the crack initiation sites. Thermo-mechanical simulations were done to analyse the stress field. Crack initiation at mid-height, from the center of the specimens was predicted, in accordance with the observations. The pore-induced stress concentration was found to depend on the local stress triaxiality, as well as K_I for an annular crack initiated from a pore.*

INTRODUCTION.

Blocks of vitrified nuclear waste for deep underground storage are prepared by pouring a mixture of waste with molten sodium-borosilicate glass into steel canisters. During cooling, sharp temperature gradients produce tri-axial tensile stresses, responsible for multiple cracking. When stored underground for hundreds of years, the canisters might not remain water-tight, allowing leaching of the fractured glass by water and the release of radionuclides in the environment. Crack initiation and growth in cylindrical specimens of an inactive analogous glass during “cold-to-hot” thermal shocks that induce a triaxial tension field representative of the loading conditions during glass blocks cooling was thus investigated.

EXPERIMENTAL AND NUMERICAL PROCEDURES

Experimental procedures.

The material investigated is a non-translucent SON68 glass, an inactive analogue of the industrial product, containing mainly SiO_2 (45,5weight %), B_2O_3 (14%), Na_2O (9,9%), many other oxides, plus Ruthenium and Palladium particles, to replace some heavy radionuclides. It is flawless, thanks to a slow cooling process, but, like the industrial glass, it contains a distribution of more or less spherical pores, issued from gas bubbles trapped in the solidifying liquid, whose diameter ranges from 100 to 800 μm . The thermo-elastic properties were measured between 20°C and the glass- transition temperature, which is 502°C [1]. Relaxation tests have shown that below 350°C, viscous effects are negligible during the short time fracture tests reported below.

36 to 45mm-high and 80mm-high cylinders, 40mm in diameter were machined. These cylinders were equipped with three thermocouples glued in the center of each base and on the side, at mid-height. They were cooled in a freezer during more than 12h and then submitted to

a “cold-to-hot” thermal shocks, by quenching it into an oil bath pre-heated at a temperature ranging from 290 to 320°C. During quenching, the specimens were kept vertical, so as to preserve the axial symmetry of the thermal and mechanical fields. The signals from the three thermocouples were recorded, to be used as boundary conditions in finite element simulations. After the thermal shocks, longitudinal and transverse sections were prepared for some observations of damage with an optical digital microscope, also used for fractographic observations of broken specimens.

Numerical procedures

An axisymmetric F.E. model was developed to simulate the thermal shocks, with 0.2mm*0.2mm-large quadratic elements at mid-height along the symmetry axis and a progressive enlargement towards the upper/lower face and the outer surface, where the element size was 1*1mm. Figure 1 shows the corresponding mesh and the position of four elements, denoted by A, B, C and D, where the evolution of stresses has been analysed in detail. Point A is near the upper edge, point B is more inside the specimen, point C is at mid-height and mid radius, while point D is at the center of the specimen.

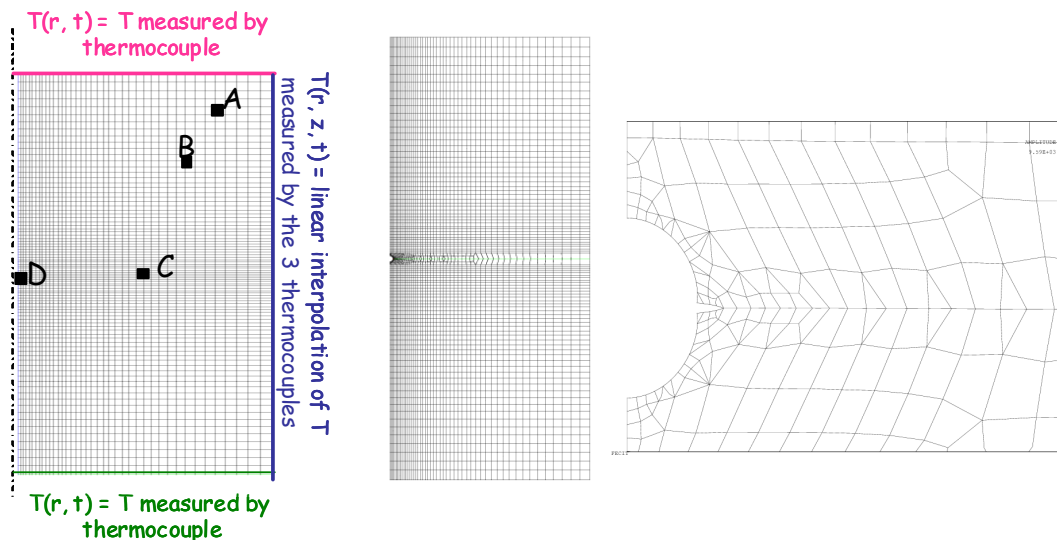


Figure 1: a) Axisymmetric F.E. model used to simulate the thermal shocks
 b) cylinder with an annular crack initiated from a spherical pore c) detail

Starting with a uniform temperature of -20°C, a 5-minute period in air was first simulated, to take into account the time needed to take the specimen out of the freezer and prepare it for oil quenching. During this period, convective heat transfer with air at 20°C, with a convection coefficient of $10\text{Wm}^{-2}\text{k}^{-1}$ was simulated along the external boundaries. This period had a very limited influence on the temperature field, since the outside temperature raised by 3 to 5°C at most, while the inside temperature remained unchanged. Then the temperature evolutions captured by the thermocouples glued on the upper and lower face during quenching were imposed along these faces, while the temperature captured by the thermocouple at mid-height was imposed there. For the other points along the side surface, a linear interpolation between the three signals was made. The influence of temperature on the elastic and thermal properties of the glass was taken into account, as detailed in [1].

Some simulations of thermal shock were also done with an annular crack initiated from a central pore, at mid-height (figure 1b and c). The stress intensity factor was computed, using the G-theta method, for various pore sizes and various crack lengths

The influence of stress triaxiality on the stress concentration near a spherical pore was investigated, using the finite element model shown on figure 2a, representing one eighth of a pore in a cube (5 times as large as the radius of the hole) with symmetry conditions enforced on the three faces that cut the pore and uniform stresses applied in one, two or three directions, as illustrated by the colored arrows.

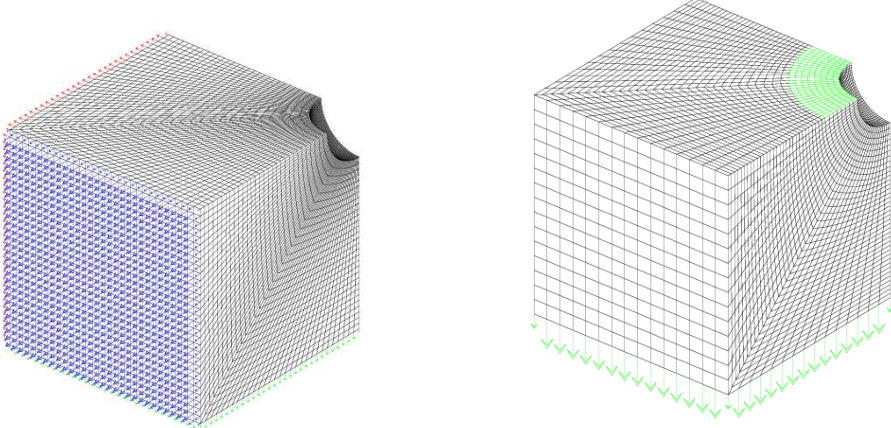


Figure 2: Models used to compute a) the stress concentration near a spherical pore b) K_I along the front of an annular crack initiated from a pore under uniaxial, biaxial or triaxial tension

The stresses along the edges cutting the pore were extracted and the stress concentration deduced from the values in the first element near the pore. The influence of stress triaxiality on the stress intensity factor for an annular crack initiated from the pore was investigated, using the mesh shown on Fig. 2b.

EXPERIMENTAL RESULTS AND NUMERICAL ANALYSIS

Preliminary computations.

Figure 3 shows the contours of the first principal stress at three moments of a thermal shock with $\Delta T=294^\circ C$. A weak tension first appears near the edges of the specimen at 45° to the symmetry axis, then the tension peak is progressively displaced towards the inside and rises. Finally the maximum tension occurs at mid-height on the symmetry axis.

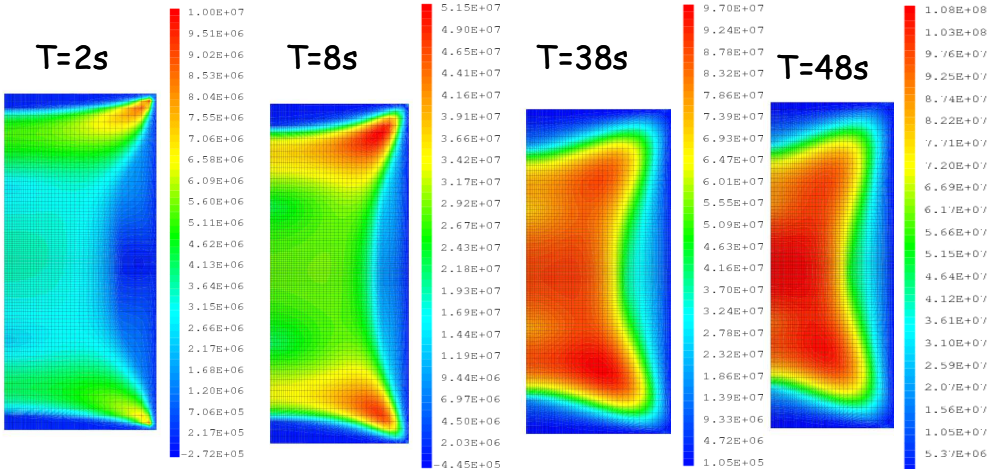


Figure 3: contours of the first principal stress at various moments of a shock

More precisely, the evolution of the three principal stresses have been computed at four places in the cylindrical specimen, denoted by A, B, C, D (see fig 1a) and are plotted on fig 4.

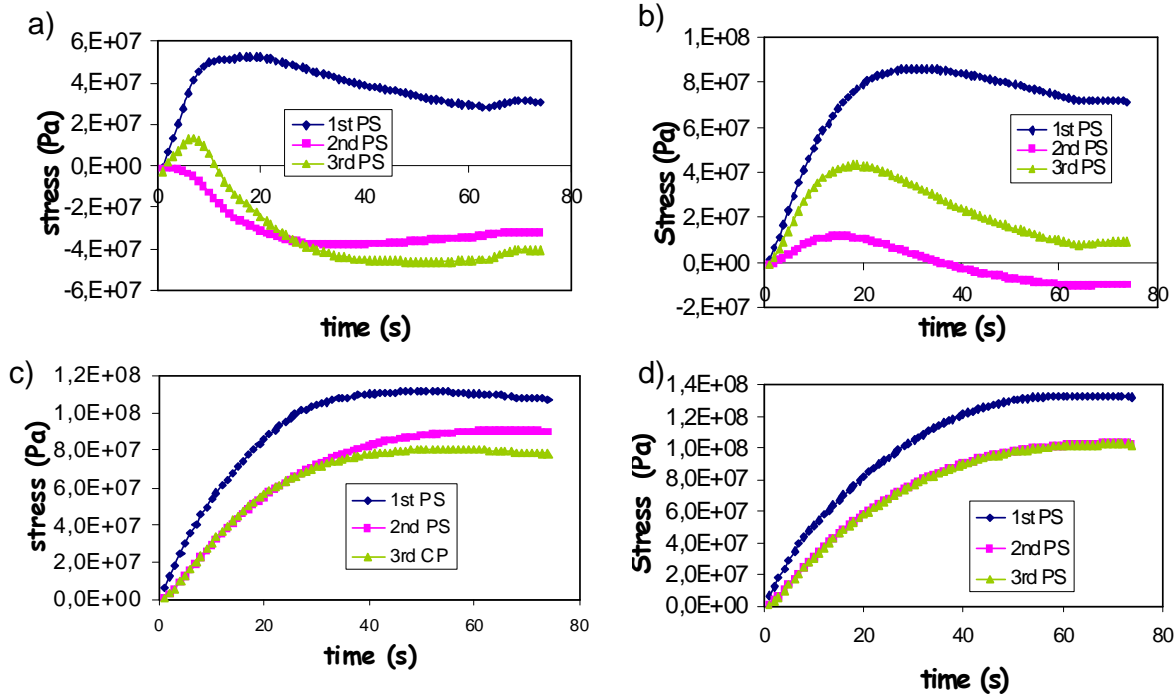


Figure 4: evolution of the three principal stresses at points A, B, C, D for $\Delta T=344^{\circ}\text{C}$

Peak stresses occur earlier near a free surface - where loading is non-proportional- but are smaller than at points located deeper inside. Near the center-point, loading is proportional and the principal directions are r , θ and z . The stress state and triaxiality are quite different from one place to the other. Only one principal stress is always positive at point A, two at point B, while points C and D experience triaxial tension all the time. The stress concentration near the pores thus varies, depending on their position in the specimen, as shown below.

Goodier [2] provided analytical expressions of the stresses near a spherical pore in an elastic infinite medium under uniform loading. For a Poisson's ratio $\nu=0.3$, the stress concentration factor near a pore is 2.04, 1.36 and 1.5 for uniaxial, equibiaxial and equitriaxial tension, respectively. But these results are not valid near the edges of specimens in which stress gradients exist. The stress concentration near pores in the specimens was thus evaluated numerically, by applying the three principal stresses computed at A, B, C or D at peak value of the first principal stress in flawless glass on the boundary of the F.E. model shown on Fig 2a. Figure 5 compares the evolution of the first principal stress at A, B, C and D. The stress concentration factor, K_t induced by a pore at each point is also indicated, as well as the resulting local stress (K_t times the peak value of the first principal stress).

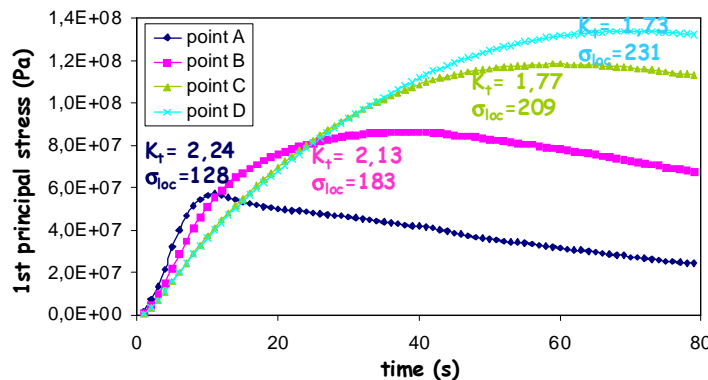


Figure 5: Compared evolution of the first principal stress and of K_t at points A, B, C, D

K_I was found to decrease from 2.24 to 2.13, 1.77 and finally 1.73, going from point A to point D. Pores should thus be less detrimental under triaxial than uniaxial loading. This is confirmed by the comparison of the stress intensity factors computed for an annular crack initiated from a pore under uniaxial, biaxial or triaxial tension (figure 6).

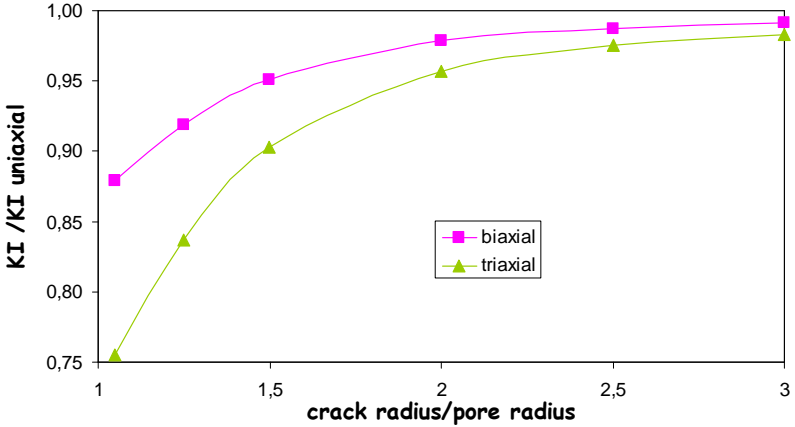


Figure 6: Influence of triaxiality on K_I for an annular crack initiated at a pore.

But even taking into account the potential presence of a pore at A, B, C or D, the local amplified stress is still predicted to increase from 128 to 183, 209 and finally 231MPa (fig. 5). Damage initiation, is thus expected near the center of the cylinders, if pores can be considered as isolated.

A change in height of the specimens, for fixed thermal boundary conditions, changes the stress state in the critical area, as illustrated on figure 7. For short specimens ($H < 36\text{mm}$), the radial and hoop stresses are predominant in the center (fig 7a) and vice versa for high specimens (fig 7b). Upward thermal shocks on cylinders thus constitute a convenient way to apply triaxial tension to a brittle material, with a possibility to vary the relative proportion of axial, radial and tangential stresses by changing the height-to- diameter ratio of the specimens.

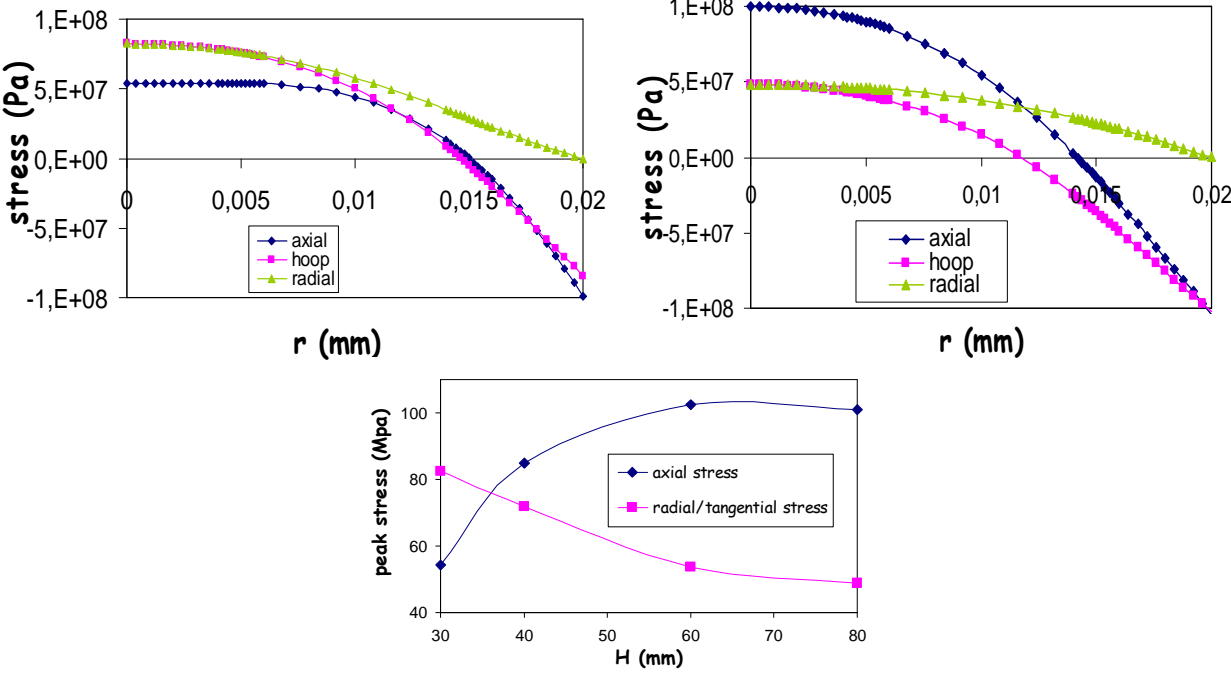


Figure 6: Radial stress profiles at mid-height for a) $H=30\text{mm}$ and b) $H=80\text{mm}$. C) Peak stresses as a function of H .

Experimental results and discussion

The condition and results of the thermal shocks are summarized in Table 1 where the height of the specimens, the amplitude of the thermal shock and the peak first principal stress at the center-point, D, are indicated.

Table 1: results of thermal shock experiments

Test n°	12	6	8	2	7	10	9	5	11	4
H (mm)	45	36.6	45	40.4	40.5	45	45	45	45	44.6
ΔT (°C)	286	314.5	291.3	327.3	322.8	301	320	344.5	296	341.9
damage	none				Micro cracks	Fracture from the bulk			Edge scaling from pore clusters	
peak P.S. at D Mpa	90	90,5	97.1	101.3	99.4	100.5	105.5	112.5	98.7	113.4

A transition from “no damage” to complete fracture in many pieces with a strong audible noise occurred within a quite narrow range of peak tensile stress in the center (a parameter more pertinent than the thermal amplitude to compare specimens with different heights). No damage was detected for a peak principal stress below 98MPa, while specimens loaded above 105MPa fractured. Between these two values, specimen to specimen variations were observed and seem to be related to the heterogeneity of pore distributions.

One of the most severe thermal shocks (unfortunately on a thermo-couple-free specimen) induced a complex internal 3D star-like crack pattern, with a typical “mirror, mist and hackles” pattern at mid-height along the symmetry axis at the initiation site, as illustrated by figure 7. The mirror zone was 2.5mm in diameter and surrounded two pores responsible for crack initiation. Beyond this flat zone, crack segmentation into a very large number of tilted and slanted parts occurred. Note that the bifurcation point does not coincide with the change from a predominant axial stress to a predominant tangential or radial stress, which occurs for a much larger radius (see fig 6b).

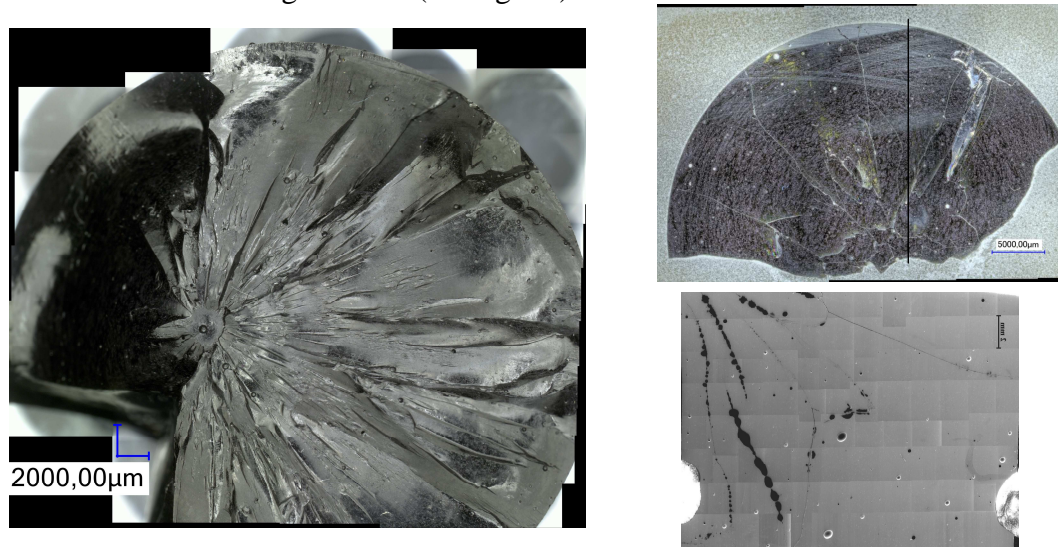


Figure 7: fractured specimen due to a thermal shock with $\Delta T= 310^{\circ}\text{C}$ a) main fracture b) transverse section c) longitudinal section along the line drawn in b)

The reasons for the transition from the mirror (a single, penny-shape crack) to the mist and then hackles pattern have been discussed by many authors [3-4] and lie in the dynamic character of crack growth in brittle materials. Above a given crack growth rate, the direction

of maximum hoop stress $\sigma_{\theta\theta}(r,\theta)$ ahead of the tip does not correspond to $\theta=0$ any more, but to a finite angle, which depends of the crack growth rate [5]. In addition as the crack velocity approaches its terminal value (a fraction of Rayleigh waves speed) energy dissipation by the acceleration of a single crack becomes insufficient and segmentation into many cracks occurs.

The stress intensity factor for a crack initiated from a pore, at mid-height of a cylinder, during such a thermal shock has been computed for various pore sizes and various crack lengths. The results are plotted as a function of time on fig. 8a, while fig. 8b shows the peak value of K_I as a function of the crack length.

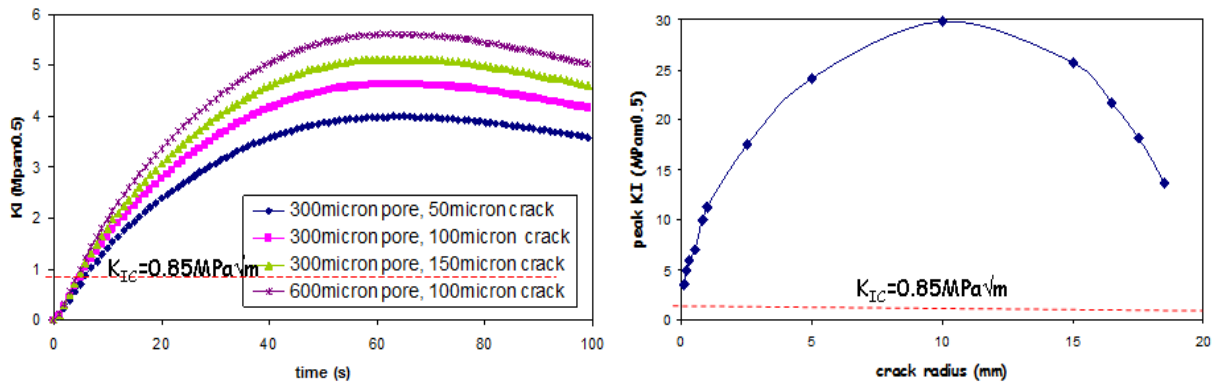


Figure 8: a) K_I for a crack initiated from a pore, at mid-height of a cylinder, for $\Delta T=291.3^\circ\text{C}$
 b) peak value of K_I as a function of the crack length for $\Delta T=341.9^\circ\text{C}$.

K_I exceeds K_{Ic} ($0.85 \text{ MPa}\sqrt{\text{m}}$) very early, for very small cracks and the crack driving force keeps on increasing with the crack length, until its radius reaches 10mm, so that a sharp acceleration should occur. Dynamic effects can indeed be expected.

An additional reason can however be put forward for the observed tilting and twisting of the crack: due to the triaxial tension in the specimen, the crack experiences two positive T-stresses: one parallel to its front: σ_r and one tangential, $\sigma_{\theta\theta}$. Such positive non-singular stresses are known to make the straight crack path unstable [6]. The former should favour crack tilting and the latter crack twisting.

Fracture also occurred for test n° 5, but in that case, two crack initiation sites were identified. A pore gave rise to a penny-shape crack, 3.67mm in diameter (fig. 9a) inclined by 35° with respect to the axis. A more or less circular “mirror zone” with a similar diameter, almost normal to the axis, but somewhat shifted from the center and from the mid-height plane, was also observed (figure 9b). Many secondary cracks were observed on a longitudinal section (fig. 9c)

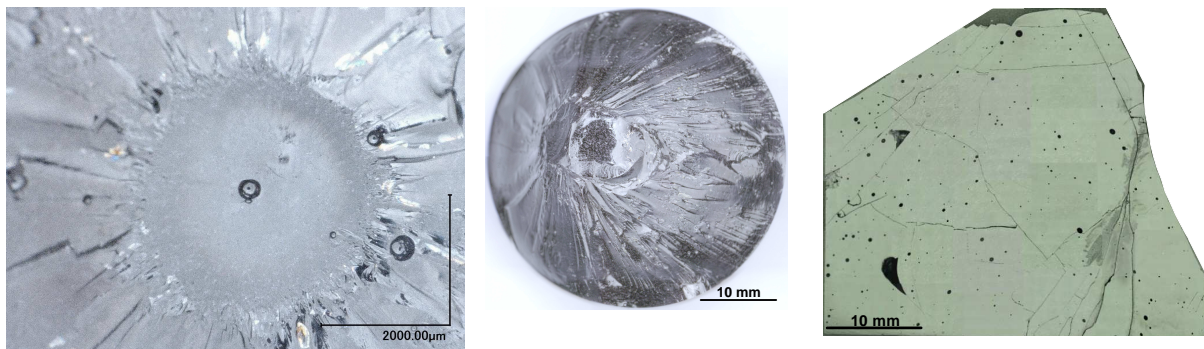


Figure 9: Broken specimen n°5 ($\Delta T=344.5^\circ\text{C}$) a) “mirror- mist-hackles” zone at a secondary crack initiation site b) Main fracture surface c) longitudinal section

Scaling at nearly 45° to the axis, near the upper or lower edges occurred in some specimens. Fractographic observations (Fig.10) revealed that pore clusters were responsible for this kind of damage. Finite element computations confirmed that stress concentrations in-between neighbouring pores are higher than near an isolated pore and rise as the distance between the pore decreases.

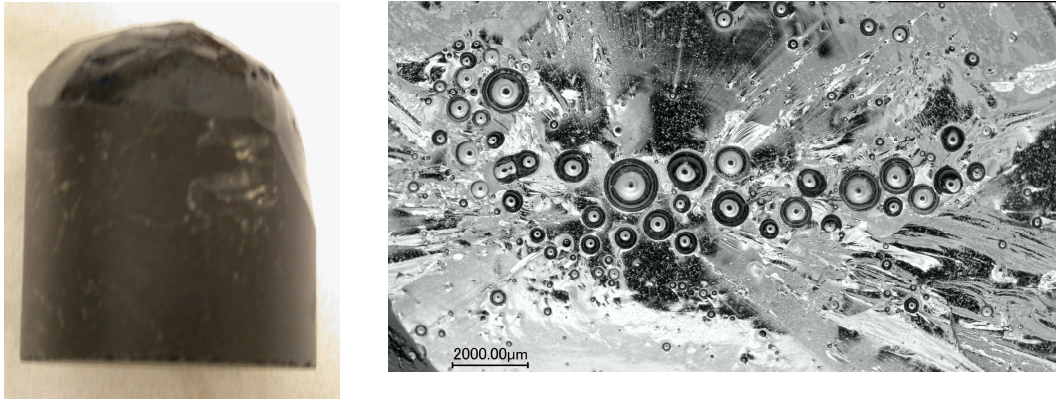


Figure 10: Scaled specimen n°7 a) side view b) pores cluster at the origin of scaling

An increase in the number of fragments was noticed as the thermal amplitude increased. Work is now in progress to measure approximately the free surface exposed by fracture for each specimen and to compare it with predictions based on a Griffith-style approach, after computation of the peak elastic energy associated with the transient stresses and strains. Such an approach was successfully applied previously to analyse the damage induced by “hot-to-cold” thermal shocks inducing biaxial tension in thin disks of the same glass [1].

CONCLUSIONS

“Cold-to-hot” thermal shocks on cylinders constitute a convenient way to apply triaxial tension to a brittle material, with a possibility to vary the relative proportion of axial/radial/tangential stresses by changing the height-to-diameter ratio of the specimens.

Pores in a brittle material are more or less detrimental, depending on load triaxiality. It is less harmful under triaxial tension than under biaxial or uniaxial tension.

The dynamic character of fracture in glass, responsible for fragmentation makes crack path predictions impossible from a quasistatic analysis of the stress field. However, previous work suggests that the developed surface of the crack might be estimated from the elastic energy associated with the transient stresses and strains. Such an estimate will be attempted and compared to on-going measurements of the total surface of glass fragments.

REFERENCES

1. Dube M, Doquet V, Constantinescu A, George D, Remond Y, Ahzi S (2010) *Mechanics of Materials*, **42**, 863–872
2. Goodier J.N. (1933) *Trans. ASME* Issue **APM-55-7**,
3. Rabinovitch A, Bahat D (2008), *Phys. Rev.* **E78**, 067102-1 to 067102-4
4. Cramer T, Wanner A, Gumbsch P (2000) *Phys. Rev. Letters*, **85** n°4, 788-791
5. Yoffe E.H (1951), *Phil. Mag* **42** n°330,739-750
6. Cotterell B, Rice J.R. (1980), *Int. J. Fracture*, **16** n°2, 155-169